

Short communication

Preparation of LiMn_2O_4 thin-film electrode on $\text{Li}_{1+x}\text{Al}_x\text{Ti}_{2-x}(\text{PO}_4)_3$ NASICON-type solid electrolyte

Kaoru Dokko^{a,b,*}, Keigo Hoshina^a, Hiroyuki Nakano^a, Kiyoshi Kanamura^{a,b}

^a Department of Applied Chemistry, Graduate School of Urban Environmental Sciences, Tokyo Metropolitan University, 1-1 Minami-ohsawa, Hachioji, Tokyo 192-0397, Japan

^b CREST, Japan Science and Technology Agency, 4-1-8 Honcho, Kawaguchi, Saitama 332-0012, Japan

Available online 28 June 2007

Abstract

An interface consisting of LiMn_2O_4 thin-film (1 μm thick) electrode and $\text{Li}_{1+x}\text{Al}_x\text{Ti}_{2-x}(\text{PO}_4)_3$ -based NASICON-type solid electrolyte (LTP) was prepared by a sol–gel coating method. The submicron-sized pores were involved in the thin film, and the porosity of the film was relatively high. The prepared solid–solid electrochemical interface was evaluated by cyclic voltammetry and galvanostatic charge–discharge test. Two reversible redox peaks were observed at 4.0 and 4.1 V versus Li/Li^+ in the cyclic voltammogram due to the redox of $\text{Mn}^{3+/4+}$. The LiMn_2O_4 thin-film electrode on LTP exhibited a discharge capacity of 80 mA h g^{-1} at 0.1 C rate.

© 2007 Elsevier B.V. All rights reserved.

Keywords: All solid-state; Lithium batteries; Sol–gel; LiMn_2O_4

1. Introduction

All solid-state lithium batteries consisting of solid electrodes and Li^+ ion conductive ceramic electrolyte are attractive because of no leak of electrolyte and no flammability [1]. Lithium ion conductivity of over 10^{-3} to 10^{-4} S cm^{-1} is required for practical rechargeable lithium batteries. Fortunately, some of inorganic materials show such a high ionic conductivity. For example, $\text{Li}_{0.35}\text{La}_{0.55}\text{TiO}_3$ with a perovskite structure [2,3] and $\text{Li}_{1+x}\text{Al}_x\text{Ti}_{2-x}(\text{PO}_4)_3$ with a NASICON-type structure [4–8] have been reported in literatures. The $\text{Li}_{1+x}\text{Al}_x\text{Ti}_{2-x}(\text{PO}_4)_3$ glass-ceramic is composed of grains and grain boundaries which consist of crystal and glassy components, respectively [7,8]. Li^+ ion conductivity in the glassy component is not so low compared with that in crystal bulk. This property may be suitable as a solid electrolyte for all solid-state rechargeable lithium batteries. In fact, Weppner and co-workers have already prepared an all solid-state battery of $\text{Li}_4\text{Ti}_5\text{O}_{12}/\text{Li}_{1.3}\text{Al}_{0.3}\text{Ti}_{1.7}(\text{PO}_4)_3/\text{LiMn}_2\text{O}_4$, and it was operated successfully at room temperature [9].

In this study, LiMn_2O_4 thin-film electrode was prepared on $\text{Li}_{1+x}\text{Al}_x\text{Ti}_{2-x}(\text{PO}_4)_3$ solid electrolyte using a sol–gel method. LiMn_2O_4 is one of promising cathode materials for all solid-state rechargeable lithium ion batteries, because the expansion and shrinkage of lattice constant of LiMn_2O_4 are very small during Li^+ ion insertion and extraction [10]. So far, thin-film type all solid-state lithium batteries have been prepared using sputtering [11] and pulsed laser ablation (PLD) [12]. The sol–gel method is also well known as one of promising thin-film preparation methods with some advantages, such as low fabrication cost, easy stoichiometry control, and fast deposition rate. We have already successfully prepared $\text{Li}_4\text{Ti}_5\text{O}_{12}$ thin-film electrode on a $\text{Li}_{1+x}\text{Al}_x\text{Ti}_{2-x}(\text{PO}_4)_3$ solid electrolyte using poly(vinylpyrrolidone) (PVP) sol–gel method [13]. Here, a sol–gel method with PVP was utilized for the fabrication of LiMn_2O_4 film on $\text{Li}_{1+x}\text{Al}_x\text{Ti}_{2-x}(\text{PO}_4)_3$ -based glass-ceramic (LTP) [14,15].

2. Experimental

The LTP plate of 0.15 mm thick supplied from OHARA Inc. was used as received [8], and its ionic conductivity was ca. 1.0×10^{-4} S cm^{-1} at room temperature [13]. LiMn_2O_4 thin film was prepared on a LTP plate by using PVP sol–gel coating method according to our previous report [14,15]. The addition

* Corresponding author at: Department of Applied Chemistry, Graduate School of Urban Environmental Sciences, Tokyo Metropolitan University, 1-1 Minami-ohsawa, Hachioji, Tokyo 192-0397, Japan. Tel.: +81 42 677 2827; fax: +81 42 677 2827.

E-mail address: dokko-kaoru@center.tmu.ac.jp (K. Dokko).

of PVP ($M_w = 55,000$) was very helpful in forming a uniform sol. A molar composition of the sol for the LiMn_2O_4 was $\text{Li}(\text{CH}_3\text{COO}):\text{Mn}(\text{CH}_3\text{COO})_2 \cdot 4\text{H}_2\text{O}:\text{PVP}:\text{CH}_3\text{COOH}:\text{i-C}_3\text{H}_7\text{OH}:\text{H}_2\text{O} = 1:2:20:40:40$. The sol was served as a coating solution for LiMn_2O_4 films. Spin coating was conducted on LTP substrate under a rotation speed of 3000 rpm in order to prepare a gel film. This gel film was converted to ceramic thin film by heating at temperature of 600°C in air for 5 min. Both spin coating and heating processes were performed repeatedly, until the film thickness became $1.0\ \mu\text{m}$. After that, the thin film was heated at 600°C for 20 min. The prepared LiMn_2O_4 thin film was observed with scanning electron microscope (SEM, JSM-5310, JEOL) and field-emission scanning electron microscope (FE-SEM, JSM-6100, JEOL). The prepared thin film was characterized with X-ray diffraction (XRD, RINT-2000, Rigaku) with $\text{Cu K}\alpha$ radiation and Raman spectroscopy (NRS-1000, Jasco) with $532\ \text{nm}$ radiation.

Electrochemical measurements were performed using two-electrode configuration as reported elsewhere [13]. The working electrode was LiMn_2O_4 coated on LTP solid electrolyte. In order to obtain electrical contact from LiMn_2O_4 surface, Au thin film was fabricated on LiMn_2O_4 surface by dc-sputtering method. Counter electrode was pure lithium metal. LTP solid electrolyte contains Ti^{4+} ion as one of main chemical components, therefore, this electrolyte is easily reduced by Li metal. In order to avoid undesirable reaction between LTP and lithium metal, polymethyl methacrylate (PMMA) gel-polymer electrolyte was used as a buffer layer. The PMMA gel-polymer electrolyte was prepared by thermal polymerization [16]. Methyl methacrylate monomer (MMA) containing ethylene glycol dimethacrylate (EGMA) as cross-linking agent was polymerized in a mixed solvent of ethylene carbonate and diethyl carbonate (1:1 in volume) containing $1\ \text{mol dm}^{-3}$ LiClO_4 ($\text{LiClO}_4\text{-EC-DEC}$). Azobisisobutyronitrile (AIBN) was used as polymerization initiator. The weight ratio of MMA, EGMA, AIBN, and $\text{LiClO}_4\text{-EC-DEC}$ was 1:0.05:0.02:2.87. The polymerization was carried out in inert atmosphere at 80°C for 1 h. The thickness of the PMMA gel-polymer was $300\ \mu\text{m}$ and its conductivity was ca. $1 \times 10^{-3}\ \text{S cm}^{-1}$ at room temperature. Cyclic voltammetry (CV) was performed using a potentiostat (HSV-100, Hokuto Denko). The galvanostatic charge and discharge experiment was conducted with an automatic discharge and charge equipment (HJR-110mSM6, Hokuto Denko). Cut-off voltages were 4.3 and 3.5 V for charge and discharge processes, respectively. The impedance measurement was performed with an electrochemical measurement system (SI-1287 and 1255B, Solartron). The alternating voltage signal was 5 mV root mean square (rms) and the frequency range was from 100 kHz to 10 mHz. All electrochemical experiments were conducted in an argon-filled glove box at room temperature.

3. Results and discussion

Fig. 1 shows the XRD patterns of LTP solid electrolyte itself and the LiMn_2O_4 thin film prepared on the LTP solid electrolyte. In the diffraction pattern of Fig. 1(b), an additional

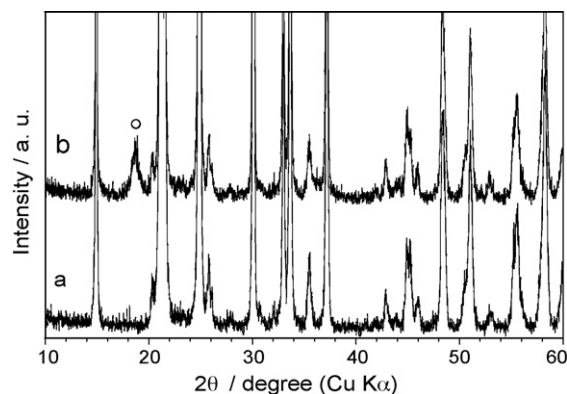


Fig. 1. XRD patterns of LTP (a) and LiMn_2O_4 thin-film fabricated on LTP plate (b).

peak was observed at $2\theta = 18.7^\circ$, which was assigned to diffraction peak from LiMn_2O_4 with spinel structure, although the peak was broad due to the relatively low annealing temperature (600°C) compared to the case of normal solid state synthesis. Fig. 2 shows the Raman spectrum of LiMn_2O_4 fabricated on the LTP plate. No impurity phase was detected by Raman spectroscopy. Factor group analysis for the cubic spinel LiMn_2O_4 with space group (O_h^7 symmetry) predicts five Raman active modes ($A_{1g} + E_g + 3F_{2g}$) [17]. The Raman spectrum of LiMn_2O_4 consists of a series of bands between 300 and $700\ \text{cm}^{-1}$. The strongest peak at $620\ \text{cm}^{-1}$ is assigned to A_{1g} mode, and the weak peaks at 380, 480, and 597 are assigned to $F_{2g}(1)$, $F_{2g}(2)$, and $F_{2g}(3)$ modes, respectively.

The morphology of surface and cross-section of the film was observed with SEM. Fig. 3 displays the SEM images of the LiMn_2O_4 prepared on the LTP substrate. The surface morphology of the LiMn_2O_4 electrode was rough. The thickness of the thin film was estimated to be $1.0\ \mu\text{m}$ from the cross-sectional view. The submicron-sized pores were involved in the thin film, and the porosity of the film was relatively high. The precursor of LiMn_2O_4 was prepared from CH_3COOLi and $\text{Mn}(\text{CH}_3\text{COO})_2$, and they remained as acetates during the gelation. During the calcination, they decomposed into manganese oxides, H_2O , and

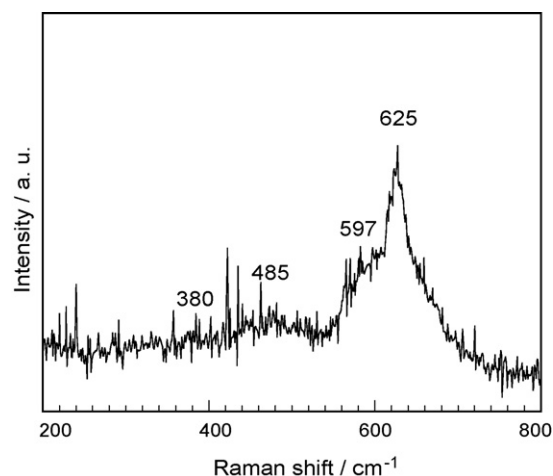


Fig. 2. Raman spectrum of LiMn_2O_4 thin-film fabricated on LTP plate.

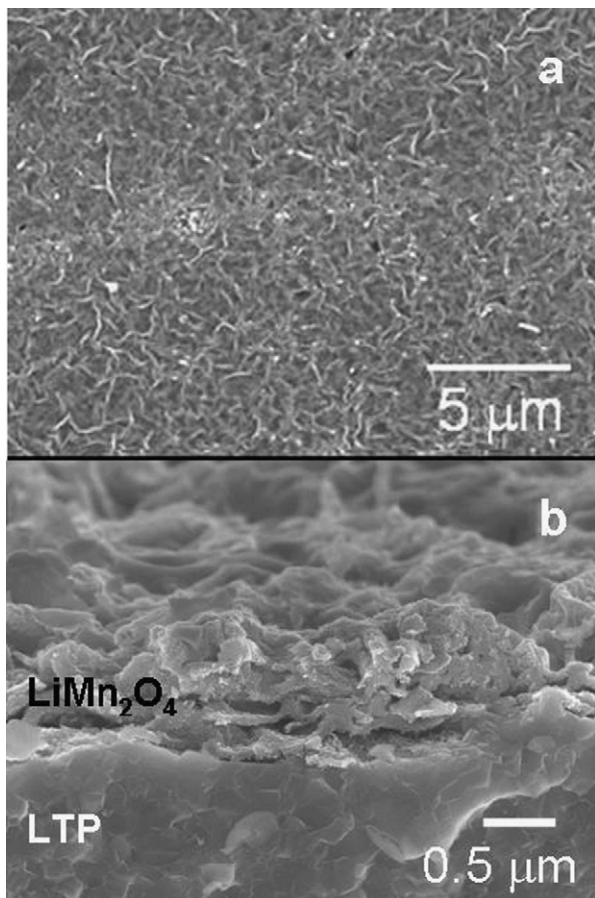


Fig. 3. SEM images of LiMn₂O₄ thin film prepared on LTP plate: (a) surface and (b) cross-section.

CO₂. The gas generation resulted in roughening the surface and forming pores.

Fig. 4 shows a cyclic voltammogram of the LiMn₂O₄/LTP/PMMA/Li cell. Despite the LiMn₂O₄ film was porous, clear voltammogram was observed. This voltammogram showed a good agreement with that of LiMn₂O₄ thin-film

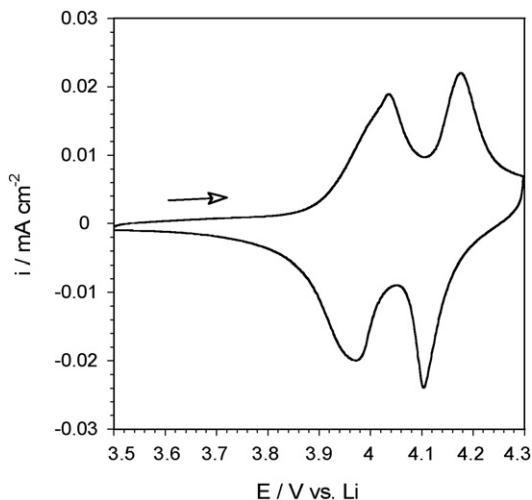


Fig. 4. Cyclic voltammogram of LiMn₂O₄/LTP/PMMA/Li cell measured at a scan rate of 0.167 mV s⁻¹.

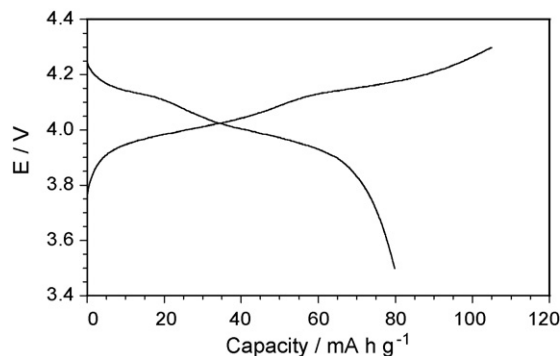


Fig. 5. Charge and discharge curves of LiMn₂O₄/LTP/PMMA/Li cell measured at 0.1 C (1 μA cm⁻²).

electrode in a liquid electrolyte reported in our previous paper [14,15]. Two reversible redox peaks were observed at 4.0 and 4.1 V, which were due to the redox of Mn^{3+/4+} in the LiMn₂O₄ spinel [10]. The reversible electrochemical behaviour suggested that the Li⁺ ion transfer between the LiMn₂O₄ electrode and LTP took place reversibly. Fig. 5 shows the charge and discharge curves of the LiMn₂O₄/LTP/PMMA/Li cell measured at 0.1 C rate (1 μA cm⁻²). Two potential plateaus at 4.0 V and 4.1 V were observed, which well correspond to the two peaks in the CV (Fig. 4). The discharge capacity of the LiMn₂O₄ was ca. 80 mA h g⁻¹, which was considerably smaller than the theoretical capacity (148 mA h g⁻¹). It was considered that some part of the film was electrically isolated due to the porous nature of the thin film. The isolated part could not participate in the redox reaction. Another possibility was formation of undetected impurities existing at the solid–solid interface or in the LiMn₂O₄ thin film. Indeed, XRD peak of LiMn₂O₄ was very weak and Raman peaks were distinguished only a part of active modes. The impurities might lead to the small discharge capacity.

Fig. 6 shows a typical Nyquist plot obtained from LiMn₂O₄/LTP/PMMA/Li cell. A depressed semicircle in the high frequency region and Warburg-type impedance in the low frequency region were observed. The depressed semicircle was attributed to the Li⁺ ion transfer at the solid–solid interface of LiMn₂O₄/LTP, and the Warburg impedance was owing to the Li⁺ diffusion in the LiMn₂O₄ thin film. The charge transfer resistance was ca. 1500 Ω cm², which was much larger than that of LiMn₂O₄ measured in liquid electrolytes [15]. It was considered that such high charge transfer resistance was caused by formation of undetected impurities existing at the solid–solid

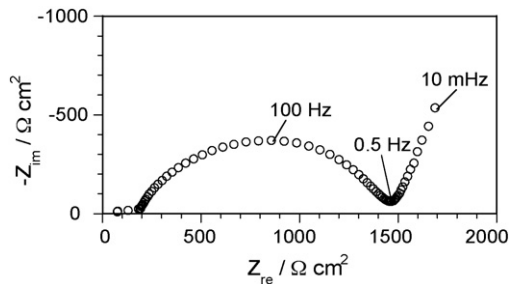


Fig. 6. Typical Nyquist plot obtained from LiMn₂O₄/LTP/PMMA/Li cell at 4.0 V.

interface and/or insufficient contact between LiMn_2O_4 and LTP. The optimization of heat treatment process for sol–gel fabrication of LiMn_2O_4 thin-film electrode is needed to reduce the charge transfer resistance and improve the electrochemical performance of the solid–solid interface between LiMn_2O_4 and LTP.

4. Conclusions

The electrochemical solid–solid interface between LiMn_2O_4 and LTP was successfully fabricated by PVP sol–gel method. Although the fabrication process of the LiMn_2O_4 thin film needs further improvements, the interface between LTP and LiMn_2O_4 fabricated by PVP sol–gel method can be applied to thin-film battery. Further efforts are underway in our group to prepare flat and dense LiMn_2O_4 thin film using the sol–gel method. If this process is carefully optimized, the solid–solid contact may be improved. This will lead to a higher electrochemical performance of the solid–solid interface between LiMn_2O_4 cathode and LTP.

Acknowledgements

The authors thank Prof. H. Masuda and Dr. K. Nishio (Tokyo Metropolitan University) for their help in taking FE-SEM photographs.

References

- [1] J.M. Tarascon, M. Armand, *Nature* 414 (2001) 359.
- [2] Y. Inaguma, C. Liqun, M. Itoh, T. Nakamura, T. Uchida, H. Ikuta, M. Wakihara, *Solid State Commun.* 86 (1993) 689.
- [3] T. Abe, M. Ohtsuka, F. Sagane, Y. Iriyama, Z. Ogumi, *J. Electrochem. Soc.* 151 (2004) A1950.
- [4] H. Aono, E. Sugimoto, Y. Sadaoka, N. Imanaka, G. Adachi, *J. Electrochem. Soc.* 137 (1990) 1023.
- [5] H. Aono, N. Imanaka, G. Adachi, *Accounts Chem. Res.* 27 (1994) 265.
- [6] X. Xu, Z. Wen, Z. Gu, Z. Xu, Z. Lin, *Solid State Ionics* 171 (2004) 207.
- [7] J. Fu, *Solid State Ionics* 96 (1997) 195.
- [8] J. Fu, *J. Am. Ceram. Soc.* 80 (1997) 1901.
- [9] P. Birke, F. Salam, S. Doring, W. Weppner, *Solid State Ionics* 118 (1999) 149.
- [10] T. Ohzuku, M. Kitagawa, T. Hirai, *J. Electrochem. Soc.* 137 (1990) 769.
- [11] B. Wang, J.B. Bates, F.X. Hart, B.C. Sales, R.A. Zuhr, J.D. Robertson, *J. Electrochem. Soc.* 143 (1996) 3203.
- [12] Y. Iriyama, T. Kako, C. Yada, T. Abe, Z. Ogumi, *Solid State Ionics* 176 (2005) 2371.
- [13] K. Hoshina, K. Dokko, K. Kanamura, *J. Electrochem. Soc.* 152 (2005) 2138.
- [14] Y.H. Rho, K. Kanamura, *J. Electrochem. Soc.* 150 (2003) A107.
- [15] Y.H. Rho, K. Dokko, K. Kanamura, *J. Power Sources* 157 (2006) 471.
- [16] S. Kuwabata, M. Tomiyori, *J. Electrochem. Soc.* 149 (2002) A988.
- [17] C.M. Julien, M. Massot, *Mater. Sci. Eng. B* 97 (2003) 217.